THE VALIDITY OF THE CONTINUUM LIMIT IN THE GRAVITATIONAL N-BODY PROBLEM

IOANNIS V. SIDERIS

Department of Physics, Northern Illinois University, DeKalb, IL 60115
sideris@nicadd.niu.edu

November 3, 2003

Abstract

This paper attempts to give quantitative as well as qualitative answers to the question of the analogy between smooth potentials and N-body systems. A number of simulations were performed in both integrable and nonintegrable smooth environments and their frozen N-body analogues, and comparisons were made using a number of different tools. The comparisons took place on both statistical and pointwise levels. The results of this study suggest that microscopic chaos associated with discreteness effects is always present in N-body configurations. This chaos is different from the macroscopic chaos which is associated with the bulk potential and persists even for very large N. Although the Lyapunov exponents of orbits evolving in N-body environments do not decrease as N increases, comparisons associated with the statistical properties, as well as with the power spectra of the orbits, affirm the existence of the continuum limit.

1 Introduction.

Simulations of the self-consistent N-body problem are desirable since they are often the most accurate numerical representations of real physical systems. However, these simulations are computationally expensive, especially when the number of particles is large. A common alternative is to study a system using a smooth, continuous potential that does not depend on time. Then, two major problems immediately emerge.

Firstly, the self-consistent N-body problem is characterized by spatial as well as temporal evolution. Therefore it generates a time-dependent potential. However, it is not clear how the temporal evolution depends on the number of particles. Different numbers of particles N may lead to different time scales in the evolution of the N-body system. In this sense it is a rather difficult task to define a smooth potential with a time dependence which can reproduce the time scales associated with the evolution of the N-body system.

Secondly an N-body system is discrete, while a smooth potential is continuous. No systematic investigation has been performed that clearly shows how granularity in the N-body system makes the dynamics of that system different from that in the smooth potential. For example a smooth potential can admit only regular orbits (when the system is integrable), while it is known that the N-body problem is always chaotic [1].

We can provide answers for the second problem to a certain extent. This is because in practice the N-body problem can be broken into two parts. (a) Generate a frozen N-body system, i.e. a system of immovable N-bodies that create a discrete field. (b) Give every particle a velocity, so that the N bodies can now move and interact with each other (this is the full self-consistent N-body problem).

We can concentrate on (a) and study the motion of test particles in the frozen N-body environment. Therefore we actually assume a frozen version of the self-consistent N-body problem and investigate it. Understandably this is a restricted version of the problem, therefore it carries with it all the disadvantages a study of a restricted problem does. On the other hand it is less complicated, so we can study isolated effects, that might not be clear through the investigation of the self-consistent problem. Besides, computationally it is much cheaper, so numerical experiments are realizable without the use of enormous computer resources.

The experimental setup is straightforward. A frozen N-body problem is associated with a discrete density, which generates a discrete potential. It is feasible to approximate this discrete density with a smooth continuous density, which then generates a smooth continuous potential. And vice versa, assuming a smooth potential one can compute the corresponding density (via Poisson's equation), and then sample it in order to transform it into N three-dimensional positions, which then define a frozen N-body system (assuming we have already defined the masses of the individual particles). Therefore a smooth potential and its corresponding frozen N-body potential can be used interchangeably.

This way we have a natural setup for comparing the motion of test particles in the two environments; the discrete and its continuous analogue. The comparison can be performed in a number of levels. Firstly pointwise: what is the visual difference of orbits starting from the same initial condition but evolved in the two different regimes (discrete and smooth)? Secondly statistically: how do the mixing properties of the two environments compare? Thirdly in respect of chaotic measures; are chaotic measures (like Lyapunov exponents and complexities associated with power spectra [2, 3]) comparable for the two cases?

The main question and purpose of this investigation has to be stated clearly; if we compare a discrete frozen N-body system with its corresponding smooth environment, what is the minimum number of particles N sufficing so the two systems are characterized by approximately the same properties in pointwise, and statistical level? Alternatively, when is the use of a smooth potential instead of its corresponding frozen N-body system justifiable?

A number of experiments has been performed attempting to give a thorough answer to this question [4, 5, 6]. The idea also has practical interest in the context of beam dynamics [7]. Still it is clear that this is only the first part of this investigation. Careful and thoughtful simulations have to be done in the future involving detailed comparisons between self-consistent N-body simulations and their corresponding time-dependent smooth environments. These numerical experiments have been left as an open question to future researchers, who will have the interest and the computational resources to perform them, so they complete the work presented here.

The truth, impregnable and inaccessible as it may seem presently, will almost certainly be explored when more powerful computer resources and advanced algorithmic techniques allow simulation of the full self-consistent N-body problem with N comparable to the number of particles in a realistic system.

2 Numerical Experiments

2.1 General Description

It is important to start with a careful definition of the term 'continuum limit.' Assume a frozen N-body system which has total mass M, and is consisted of N particles of equal mass (therefore the mass of an individual particle is $m = M/N$). The density of this frozen N-body system can be mathematically expressed by a sum of delta functions as:

$$\rho(\mathbf{r}) = \frac{M}{N}\sum_{i=1}^{N}\delta(\mathbf{r}-\mathbf{r}_i) \tag{1}$$

This density generates a discrete potential (which can be calculated via Poisson's equation):

$$\Phi_N(\mathbf{r}) = -\frac{GM}{N}\sum_{i=1}^{N}\frac{1}{|\mathbf{r}-\mathbf{r}_i|} \tag{2}$$

where G is the gravitational constant.

In numerical simulations the potential is usually replaced by:

$$\Phi_N(\mathbf{r}) = -\frac{GM}{N}\sum_{i=1}^{N}\frac{1}{\sqrt{(\mathbf{r}-\mathbf{r}_i)^2+\epsilon^2}} \tag{3}$$

where ϵ is a small number called the softening parameter and is used for two reasons: (a) to protect the simulation from overflow errors that will occur when the distance between a test particle and a frozen particle becomes too small (in this case the potential becomes too large) [8], and (b) to transform the particle into a 'superparticle', i.e. a group of many particles [9] (if two of these superparticles happen to come very close the softening parameter will simply smooth out their interaction, which is actually what should happen realistically in an environment of N superparticles).

If one increases the number of particles so $N \to \infty$ and $\epsilon \to 0$ then he moves from a discrete environment of N frozen particles, each with mass m, to a smooth environment of infinite number of particles of zero mass (since $m = M/N$). The condition $\epsilon \to 0$ is necessary since there is no softening in a smooth environment. The use of a softening parameter in N-body simulations does raise a critical question though. Large values of ϵ evidently impose an upper limit in the force a test particle experiences during its motion in the frozen N-body environment. Therefore the particle does not 'feel' the kicks by the very close encounters any more. However such kicks may change significantly the evolution of the test particle, because of the sensitivity associated with the local properties of the phase space. In simple terms large values of ϵ could and do suppress all or some of the chaos caused by the close encounters of the test particles with the frozen particles [10]. This is a numerical artifact which can be highly inconvenient when the study involves and concerns chaotic effects.

The numerical methodology followed was straightforward. First, define a potential. Second, find the density associated with this via Poisson's equation. Third sample this density in order to generate N positions in the three-dimensional configuration space. This way one eventually has a system of N bodies, characterized by a discrete density which approximates the smooth density of the continuous regime. The last step is to integrate the same initial condition(s) (test particles) in both the smooth potential and the frozen-N environment.

The main potentials we used were the following:

(a) Plummer Potential. This is a well-known potential first used in 1911 to fit observations of globular clusters [9]. This potential is integrable and therefore it admits only regular orbits:

$$\Phi_P(r) = -\frac{GM}{\sqrt{r^2+b^2}}, \tag{4}$$

where G is the gravitational constant. For the experiments performed we took $G = M = b = 1$.

(b) Three-dimensional harmonic oscillator. This is also an integrable potential, which is simple and computationally fast:

$$\Phi_E(\mathbf{r}) = \Phi_0 + \frac{1}{2}\left(\omega_a^2 x^2 + \omega_b^2 y^2 + \omega_c^2 z^2\right), \tag{5}$$

where ω_a, ω_b, and ω_c are the frequencies in the three different directions and Φ_0 is constant. The values chosen for the experiments performed were: $\Phi_0 \approx -1.00608$, $\omega_a \approx 0.4663$, $\omega_b \approx 0.5508$, and $\omega_c \approx 0.6753$.

(c) Three-dimensional harmonic oscillator plus a perturbation factor which simulates a black hole at the center of a system of mass M. Because of the perturbation this potential is nonintegrable and admits large regions of global stochasticity. It has been found that large measure of orbits in this potential are chaotic [22]:

$$\Phi_{BH} = \Phi_E - \frac{GM_{BH}}{\sqrt{r^2+\epsilon^2}}, \tag{6}$$

with M_{BH} the mass of the black hole and ϵ the softening parameter. We again took $G = M = 1$, and the values for the perturbation parameters were: $\epsilon = 10^{-3}$ and $M_{BH} = 10^{-1.5} \approx 0.0316228$. We used Φ_E as in (b).

2.2 Visual Picture and Power Spectra

Let's study first what happens in an integrable potential. The most simplistic level of comparison between the two regimes is to visually examine the evolutions of the same initial condition in the smooth potential and its corresponding N-body environment for a number of different choices of N. This comparison can be seen in Figure 1. Here the orbits were integrated in the smooth Plummer potential and its corresponding frozen N-body analogues. It is clear from first inspection, that the orbit looks very chaotic when it is integrated in a discrete environment consisting of a small number N of frozen particles, but as N increases the orbit gradually resembles the smooth characteristic (last panel). Similar information can be taken from the power spectra corresponding to Figure 1. The power spectrum for small N is characterized by many frequencies but as N increases it converges to the frequencies associated with the smooth description (Figure 2). For different initial conditions the general picture is the same and only the details change.

2.3 Lyapunov Exponents

It is obvious that Figures 1 and 2 are consistent with common sense, and agree with what one would expect. However the same is not true if we examine the average largest short-time Lyapunov exponents [11]. In order to have statistically important results the same initial condition was integrated in 20 different frozen-N configurations for every choice of N (for the same N the density was sampled 20 different times and the positions of the particles in each of the 20 configurations were different). The dependence of the average short-time Lyapunov exponent on N and ϵ can be seen in Figure 3. It is obvious from this picture that for small values of ϵ the number of particles N is not crucial for the value of the Lyapunov exponent. Surprisingly this means that in Figure 1 the orbit of panel (a) and the one of panel (g) have comparable Lyapunov exponents!

It is possible to understand at least qualitatively the physical reason for this. Integrable potentials do not exhibit chaos. Therefore all the chaos observed in their frozen N-body analogues, must be associated with discreteness effects that perturb the orbits because of close encounters. This means that the time scale for the growth of a small initial perturbation can be calculated, if we consider the tidal effects associated with two particles separated by some typical interparticle distance. The tidal acceleration is:

$$\delta\ddot{\mathbf{r}} = (\delta\mathbf{r}\cdot\nabla)\mathbf{a} \sim \frac{Gm}{r^3}\delta\mathbf{r} \tag{7}$$

where r is the separation and m the particle mass. Suppose however that:

$$r \sim n^{-\frac{1}{3}} \sim N^{-\frac{1}{3}} R_{sys} \tag{8}$$

with n the characteristic number density and R_{sys} the size of the system. It then follows dimensionally that the time scale that characterizes the interaction is:

$$t_{int} \sim \frac{1}{\sqrt{G\rho}} \tag{9}$$

which is independent of N and practically comparable to the dynamical time (also independent of N).

The general claim is that if one perturbs an orbit in an N-body environment, the time scale τ on which the separation of the perturbed from the unperturbed orbit tends to grow will not diverge (will not increase without bound) for $N \to \infty$. However there is some disagreement as to whether τ should converge toward an N-independent value [12] or whether τ should instead slowly decrease with increasing N [13].

The physiognomy of this phenomenon merits introduction of the idea of 'macrochaos' versus 'microchaos'. As 'macrochaos', we define the chaos an orbit experiences because of the global properties of a potential. Practically, this is the chaos emerging when an orbit is moving in a nonintegrable smooth potential. On the other hand as 'microchaos' we define the chaos associated with the close encounters in an N-body system. Even when an initial condition is integrated in a frozen N-body system which corresponds to a regular potential in the continuum limit, it will still experience microchaos, and its Lyapunov exponent will be larger than zero. If an initial orbit is integrated in a frozen N-body system that corresponds to a chaotic potential in the continuum limit, then the Lyapunov exponent will have contributions by both the microchaos as well as the macrochaos, but the one from microchaos is usually much bigger than the one from macrochaos.

2.4 Mixing

A statistical property of major importance for the validity of the continuum limit is the mixing of initially localized ensembles of initial conditions through global regions of phase space [14, 15, 16, 17, 18]. A critical point here is that the way the mixing of the orbits proceeds in a smooth potential depends strongly on whether the orbits are regular or chaotic. It is well-known that a localized ensemble of regular orbits will mix linearly. On the other hand, a localized ensemble of chaotic orbits (chaotic mixing) will mix exponentially. In simple terms this means that after a long time the ensemble of regular orbits will still be relatively localized in the phase space, but the orbits of the chaotic ensemble will exponentially explore all the phase space energetically available to them.

In order to investigate the mixing property we define an ensemble of initial conditions in a very localized region of the phase space. By 'localized' we mean a hypercube of typical size 0.01 in a system of typical size of the order 10. Then we integrate these initial conditions in the frozen N-body environment (for different choices of number of particles N) and in the corresponding smooth environment as well.

In order to quantify the data the evolution of the dispersion was computed. The mathematical expression for the dispersion is:

$$\sigma_r^2 \equiv \langle r^2 \rangle - \langle r \rangle^2 \tag{10}$$

where

$$\langle r^p \rangle = \frac{1}{n} \sum_{i=1}^{n} (x_i^2 + y_i^2 + z_i^2)^{\frac{p}{2}} \tag{11}$$

with $n = 800$ the number of the initial conditions comprising the ensemble.

For a regular potential (Plummer) phase mixing is linear in the smooth environment. For the frozen-N environment the evolution of the dispersion was different for different values of N. For small N the dispersion grew as $t^{1/2}$ but for larger N the dependence was linear. This is easily explainable. When N is still small discreteness effects are quite strong, so that a diffusion process ($\sim t^{1/2}$) should be expected. As N increases the frozen-N environment approaches the continuum limit and a behaviour similar to that in the smooth potential should be expected (Figure 4).

The three-dimensional harmonic oscillator plus a perturbation term is a non-integrable potential which admits a large measure of chaotic orbits. The dispersion in this case evolves roughly exponentially in time and discreteness effects only serve to accelerate this growth (Figure 5).

This exponential evolution is not the only difference from the case of regular orbits integrated in the Plummer potential. Another very important difference is that σ_r for regular orbits integrated with N as small as $10^{4.5}$ resembles the σ_r evolution in the corresponding smooth potential. Clearly, for the chaotic orbits this is no longer true; even for N as large as $10^{5.5}$ phase mixing happens much faster than in the corresponding smooth potential. The problem arising here is that it gets computationally expensive to determine the number N of frozen particles that reproduce sufficiently well the mixing property of a smooth potential. There is a solution for that.

2.5 Langevin Description

The force a test particle experiences as it moves in the frozen N-body environment is intuitively decomposed into two parts. The first is the force caused by the collective action of all the frozen particles, i.e. the bulk potential. This is equivalent to the force the particle would 'feel' in a smooth potential. However a second force is embedded in this smooth action, and this is the one generated by the close encounters. This kind of action is conceptually closer to a diffusive process. Idealistic as this assumption of two separate contributions to the force of the test particle may be, it can be used effectively for our purposes.

If we allow a test particle to evolve in a smooth potential but add to its equation of motion a random factor that represents the 'kicks' caused by the close encounters, then the orbit could be equivalent to the motion the particle performs in a frozen N-body configuration. In this context we transform the canonical equation of motion into stochastic Langevin equations [19, 20, 21] which have the following form:

$$\frac{d^2 r_a}{dt^2} = -\nabla_a \Phi - \eta \frac{dr_a}{dt} + F_a, \qquad a = x, y, z. \tag{12}$$

where η can in principle depend on $\mathbf{r}$ and $\mathbf{v}$ but for the experiments performed it had a constant value, and F_a represents a Gaussian white noise. F_a can be completely characterized by its first moment and its correlation function. Its first moment is:

$$\langle F_a(t) \rangle = 0, \qquad (a, b = x, y, z)$$

and

$$\langle F_a(t_1) F_b(t_2) \rangle = 2\eta\Theta\delta_{ab}\delta_D(t_1 - t_2), \tag{13}$$

where the "temperature" Θ is associated with internal degrees of freedom of the system.

Since the energy for the frozen-N orbits remains constant, while for the 'noisy' orbits it does not, it was nessecary to include in the numerical program an energy conservation routine that corrected the orbit slightly, renormalising the velocity at each time step by an overall factor, i.e. $\mathbf{v}(t + \delta t) \to a\mathbf{v}(t + \delta t)$ with a so chosen that $E(t + \delta t) = E(t)$.

It is obvious that larger η should correspond to smaller number N. Heuristically the two quantities are connected as follows. The value of η defines a characteristic relaxation time $t_R = 1/\eta$. In practice this is the time needed in order for significant changes in conserved quantities like energy to be observed (for a self-gravitating system). On the other hand it is well-known that discreteness effects associated with close encounters in an N-body system impose a relaxation time $t_R \propto (\ln N/N)t_D$ where t_D is the characteristic dynamical time (defined as the orbital period of the orbit). Then the proportionality relationship between the two quantities is $\eta \propto \ln N/N$ and the constant involved can be easily found through a calibration computation [22].

How do the simulations in frozen N-body environments compare to the simulations using Langevin description? It is obvious from Figure 6 (compare it to Figure 4) that for the Plummer potential there is a significant qualitative agreement between the plots describing the time evolution of σ_r in the two regimes at least for $N \geq 10^4$. For very small values of N there are differences since the frozen-N σ_r grows considerably more rapidly than the noisy one. This has probably to do with the choice of the noise. Intuitively the noise that can reproduce the 'kicks' in a frozen N-body environment with small N can not be white (white noise is a Markovian process and has no memory) but (a) it should have some memory (autocorrelation time larger than zero), therefore it should be some kind of colored noise and (b) it should depend on the spatial variables (different noise in different locations). However the disagreement for small N is not crucial for the purposes of this work. The point is that since the results by the Langevin description agree statistically with the results by the frozen N-body simulations, there is a tool that allows us to give an answer to the main question of how many frozen particles suffice so the frozen and smooth environments are equivalent.

There is also a considerable similarity for the case of chaotic orbits, as is evident from Figure 7 (compare it with Figure 5). Assuming that the correspondence between N and η can be extrapolated for larger N it follows that the number of particles required for chaotic orbits in order for the discreteness effects to be unimportant is of the order of $N \sim 10^{7.5}$. Therefore there is a crucial difference between the number N needed for chaotic ensembles ($N \sim 10^{7.5}$) and the one needed for regular ensembles ($N \sim 10^{4.5}$).

3 Conclusions

It is clear that visually individual orbits evolved in frozen N-body configurations do resemble gradually the smooth characteristic as N increases. However the Lyapunov exponents of orbits evolved in frozen-N have generally large values and they do not increase with N, even when the smooth characteristics are regular orbits.

It is clear that the Lyapunov exponents computed numerically for orbits that evolve in smooth potentials are associated with the form of the bulk potential. For the case of nonintegrable potentials the positive value of the Lyapunov exponents is associated with the macroscopic chaos, or macrochaos, generated by the bulk potential. The orbits evolving in frozen N-body environments are characterized by Lyapunov exponents that are associated with the discreteness effects, i.e. they are generated by a microscopic chaos, or microchaos. This does not mean that in the case of frozen N-body configurations associated with nonintegrable potentials there is no contribution to the destabilization of the orbit because of the action of the bulk potential (macrochaos). Simply this contribution is small compared to the contribution by the discreteness effects.

This means that if one is interested in quantifying the chaos associated with the bulk potential in an N-body system, Lyapunov exponents are not really helpful. It is true however that there are techniques that can be used to extract the macroscopic contribution of the Lyapunov exponents in N-body simulations [6]. On the other hand power spectra and chaotic measures associated with them (like the complexity), do work as expected and are very useful for quantifications of the orbits.

The mixing of initially localized ensembles of orbits is a useful property to be used for the validity of the continuum limit. It turns out that there is a dramatic difference between the number of bodies necessary in order for the continuum limit to be valid, between regular and chaotic orbits. The mixing of regular orbits is well approximated with only $10^{4.5}$ particles but the mixing of chaotic orbits needs at least $10^{7.5}$ particles.

For comparatively large N discreteness effects can be imitated by energy-conserving white noise with amplitude $\eta \propto 1/N$. This agrees with the expectation that discreteness effects can be modeled as a sequence of incoherent binary encounters. Noise can be used effectively to model both bulk statistical properties of orbit ensembles and qualitative properties of individual orbits. This means that the results of experiments based on the Langevin description (which are computationally 'cheap') can be trusted, at least as first approximation, to give important information about the validity of the continuum limit.

The final conclusion is that at least in terms of macroscopic properties the continuum limit is valid for $N \to \infty$. However, convergence towards this limit is substantially slower for frozen N-body distributions, that correspond in the continuum limit to nonintegrable potentials, and admit a significant measure of chaotic orbits, than for distributions that correspond in the continuum limit to integrable potentials.

I would like to dedicate this paper to the memory of professor Henry E. Kandrup, who was my advisor and a very good friend over a number of years. I would also like to thank Courtlandt Bohn and Jeremy McCormick for useful discussions and comments. This work was supported by Department of Education grant G1A62056.

References

[1] R. H. Miller, Astrophys. J. **140**, 250 (1964).

[2] M. Tabor, *Chaos and Integrability in Nonlinear Dynamics* (Wiley, New York, 1989).

[3] A. J. Lichtenberg and M. A. Lieberman, *Regular and Chaotic Dynamics* (Springer, Berlin, 1992).

[4] H. E. Kandrup and I. V. Sideris, Phys. Rev. **E 64**, 056209.

[5] I. V. Sideris and H. E. Kandrup, Phys. Rev. **E**, Physical Review E **65**: 066203 (2002)

[6] H. E. Kandrup and I. V. Sideris, Astrophys. J., **585**: 244-250 (2003)

[7] H. E. Kandrup, I. V. Sideris, and C. L. Bohn Physical Review Special Topics - Accelerators and Beams (submitted)

[8] R. W. Hockney, J. W. Eastwood, *Computer Simulation Using Particles* (Philadelphia : A. Hilger, 1988).

[9] J. Binney and S. Tremaine, *Galactic Dynamics* (Princeton University Press, Princeton, 1987).

[10] H. E. Kandrup and H. Smith, Astrophys. J. **374**, 255 (1991).

[11] G. Bennetin, L. Galgani, A. Giorgilli, and J. M. Strelcyn, Meccanica, **15**, 9 (1980)

[12] H. E. Kandrup, Physica A **169**, 73 (1989).

[13] J. Goodman, D. Heggie, and P. Hut, Astrophys. J. **415**, 715 (1993).

[14] M. E. Mahon, R. A. Abernathy, O. B. Bradley, H. E. Kandrup, Mon. Not. R. astr. Soc. **275**, 443 (1995).

[15] H. E. Kandrup, Mon. Not. R. astr. Soc. **301**, 960 (1998).

[16] H. E. Kandrup, I. V. Pogorelov, and I. V. Sideris, Mon. Not. R. astr. Soc. **311**, 719 (2000).

[17] M. Valluri and D. Merritt, in *The Chaotic Universe*, ed. R. Ruffini and V. G. Gurzadyan (World Scientific, New York, 1999).

[18] C. L. Bohn, H. E. Kandrup, and R. A. Kishek, *Proceedings of Snowmass 2001*, ed. C. M. Sazama eConf C01/06/30, M302 (2001).

[19] S. Chandrasekhar, Rev. Mod. Phys. **15**, 1 (1943).

[20] S. Chandrasekgar, *Principles of Stellar Dynamics* (University of Chicago, Chicago, 1943).

[21] N. G. van Kampen, *Stochastic Processes in Physics and Chemistry* (North Holland, Amsterdam, 1981).

[22] H. E. Kandrup and I. V. Sideris, Celestial Mechanics, **82**, 61 (2002).

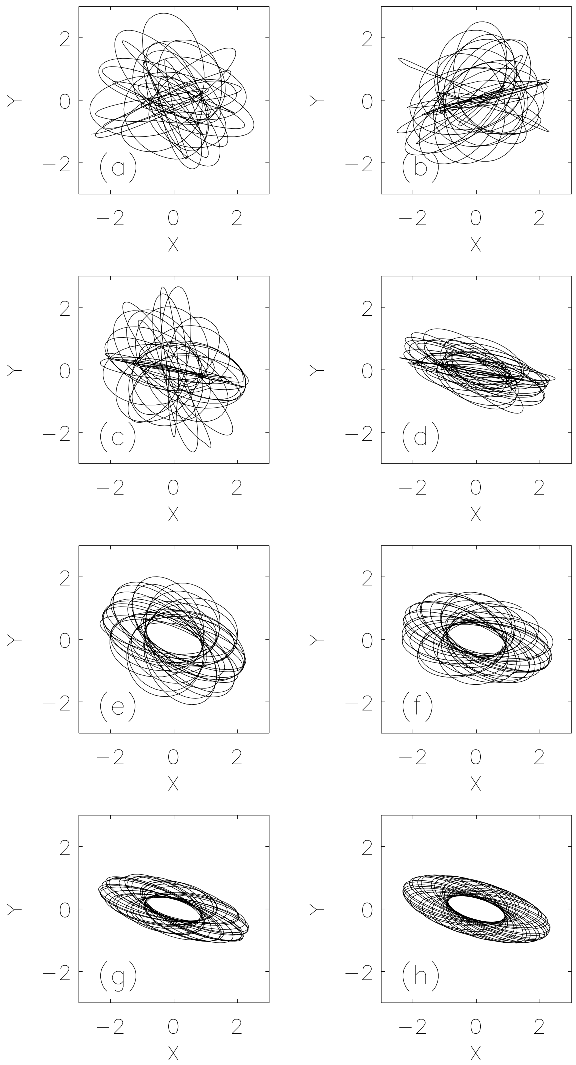

Figure 1: The x-y projection of orbits starting from the same initial condition and evolving in frozen N-body environments (corresponding to the smooth Plummer potential), for $t = 25t_D$ with $\epsilon = 10^{-5}$. (a) $N = 10^{2.5}$. (b) $N = 10^3$. (c) $N = 10^{3.5}$. (d) $N = 10^4$. (e) $N = 10^{4.5}$. (f) $N = 10^5$. (g) $N = 10^{5.5}$. (h) The x-y projection of the same initial condition evolved in the smooth Plummer potential.

.

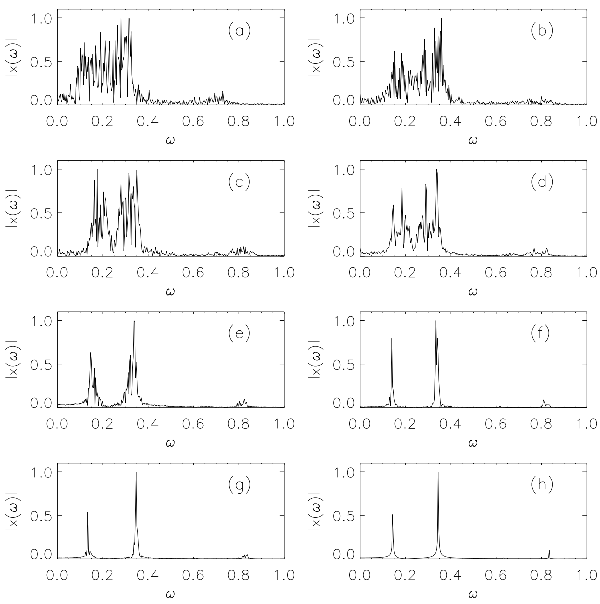

Figure 2: (a) The Fourier transformed $|x(\omega)|$ for one frozen N-body integration of the initial condition used to generate Figure 1, evolved with $\epsilon = 10^{-5}$ and $N = 10^{2.5}$. (b) The same for $N = 10^3$. (c) $N = 10^{3.5}$ (d) $N = 10^4$. (e) $N = 10^{4.5}$. (f) $N = 10^5$. (g) $N = 10^{5.5}$. (h) $|x(\omega)|$ for a characteristic in the smooth potential with the same initial condition, with data recorded at the same intervals for the same total integration time.

.

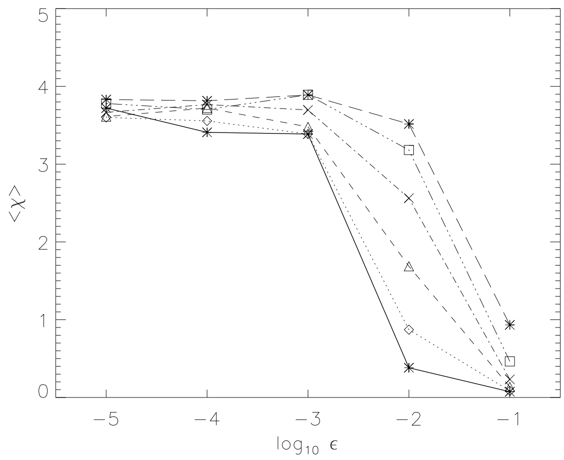

Figure 3: Average short-time Lyapunov exponent $\langle \chi \rangle$ as a function of the softening parameter ϵ for $N = 10^5$ (solid line), $N = 10^{4.5}$ (dotted), $N = 10^4$ (dashed), $N = 10^{3.5}$ (dot-dashed), $N = 10^{3.0}$ (triple-dot dashed), and $N = 10^{2.5}$ (broad dashed).

.

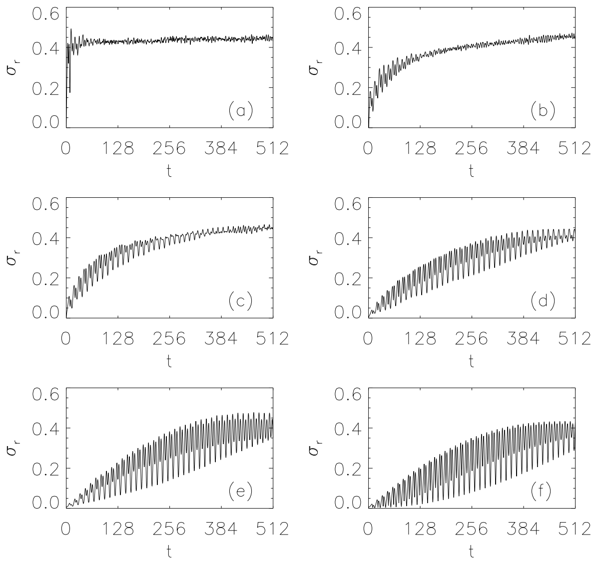

Figure 4: The dispersion σ_r associated with an initially localized ensemble of initial conditions, evolved in frozen N-body realizations of the integrable Plummer potential for variable N. (a) $N = 10^3$. (b) $N = 10^{3.5}$. (c) $N = 10^4$. (d) $N = 10^{4.5}$. (e) $N = 10^5$. (f) Evolution in the smooth potential.

.

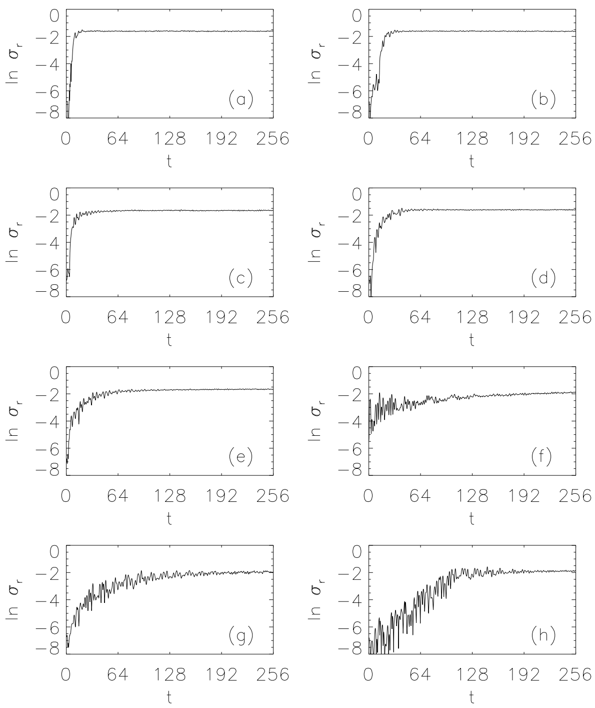

Figure 5: The dispersion σ_r associated with an initially localized ensemble of chaotic orbits evolved in frozen-N realization of the nonintegrable three-dimensional harmonic oscillator plus a perturbation term potential for variable N. (a) $N = 10^{2.5}$. (b) $N = 10^3$. (c) $N = 10^{3.5}$. (d) $N = 10^4$. (e) $N = 10^{4.5}$. (f) $N = 10^5$. (g) $N = 10^{5.5}$. (h) Evolution in the smooth potential.

.

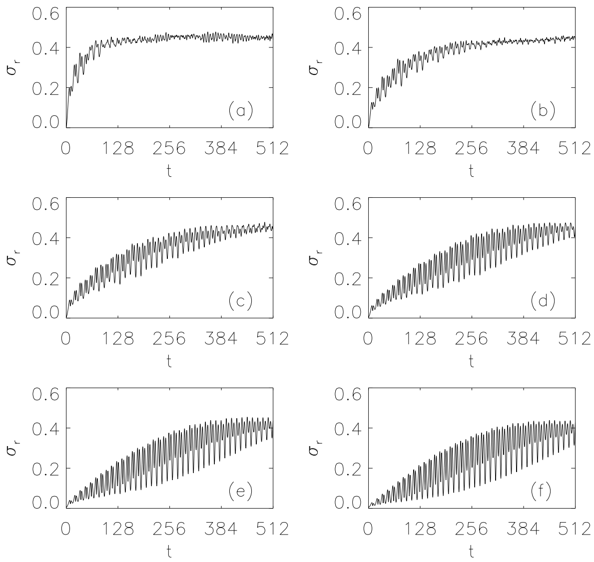

Figure 6: The dispersion σ_r associated with an initially localized ensemble of regular orbits evolved in the presence of noise in the smooth Plummer potential, for $\Theta = 1.0$ and variable η. (a) $\eta = 10^{-3}$. (b) $\eta = 10^{-3.5}$. (c) $\eta = 10^{-4}$. (d) $\eta = 10^{-4.5}$. (e) $\eta = 10^{-5}$. (f) $\eta = 10^{-5.5}$.

.

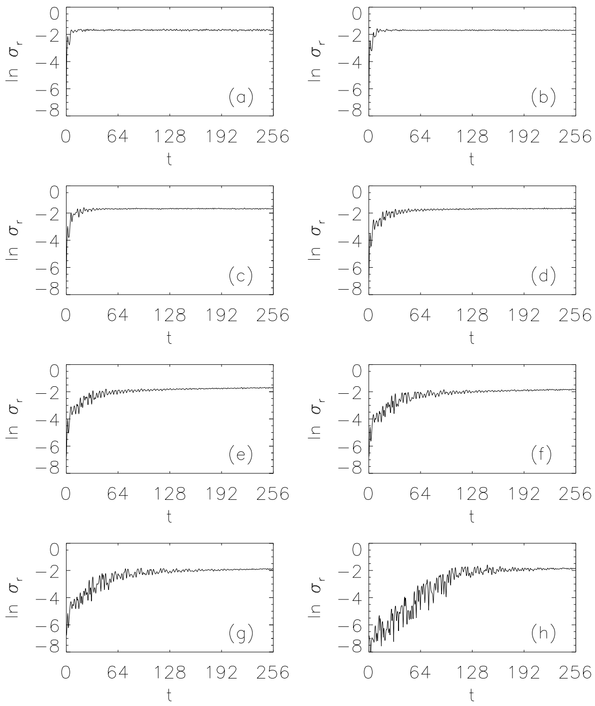

Figure 7: The dispersion σ_r associated with an initially localized ensemble of chaotic orbits evolved in the presence of noise in the smooth ellipsoid potential plus a perturbation factor for $\Theta = 1.0$ and variable η. (a) $\eta = 10^{-2.0}$. (b) $\eta = 10^{-2.5}$. (c) $\eta = 10^{-3.0}$. (d) $\eta = 10^{-3.5}$. (e) $\eta = 10^{-4.0}$. (f) $\eta = 10^{-4.5}$.(g) $\eta = 10^{-5.0}$. (h) $\eta = 10^{-7.5}$.

.